

Automatic Differentiation for Inverse Problems with Applications in Quantum Transport

1st Ivan Williams

*Electrical and Computer Engineering
University of Massachusetts Amherst
Amherst, United States
inwilliams@umass.edu*

2nd Eric Polizzi

*Electrical and Computer Engineering, Mathematics
University of Massachusetts Amherst
Amherst, United States
epolizzi@engin.umass.edu*

Abstract—A neural solver and differentiable simulation of the quantum transmitting boundary model is presented for the inverse quantum transport problem. The neural solver is used to engineer continuous transmission properties and the differentiable simulation is used to engineer current-voltage characteristics.

Index Terms—QTBM, PINN, AD, SciANN, JAX

I. INTRODUCTION

THE modern engineering design process is largely guided by computational models. Devices and systems are often first prototyped 'in-silico'. While standard numerical techniques, such as finite-element, have served well in the forward case, other computational tasks, such as model inversion, remain challenging.

Physics-informed machine learning is a mesh-free method for solving differential equations. By embedding the governing equations and boundary conditions of a physical system into the loss function of a neural network, the network can be trained to approximate the solution to the system to a high accuracy [1].

The physics-informed approach allows the solving of a physical model from a symbolic specification. This enables two important applications for computational modeling in engineering; solving models in parameter space and solving inverse and ill-posed problems.

The aforementioned advantages make the physics-informed approach well suited for problems in quantum transport. In the quasi-static approximation of quantum transport, the system energy is taken as a parameter. Using physics-informed neural networks, the solution to the quantum transmitting boundary problem is solved for every energy in a given range simultaneously allowing for the direct evaluation of transmission properties. Further, the internal potential can be represented as a neural network as well, and it can be trained to reproduce specified transmission properties (this work).

Despite the advantages of the physics-informed approach. These techniques are often affected by problems of spectral bias and stiffness [2]. Steep gradients in the true solution confound the NN and require very fine-step size and/or long training times. This is why physics-informed approaches often incorporate data and require significant computational resources.

Underpinning the physics-informed approach is automatic differentiation (AD) which allows for the optimization of the network under the constraints of the physical system. It's possible to combine the advantages of numerical linear algebra with the physics-informed approach utilizing AD tools directly [3]. Algorithms specifying matrix computations and other numerical techniques can be differentiated with respect to their parameters thus algorithms specifying approximate physical solutions can be differentiated with respect to parameters of the physical system.

The differentiable approach is well suited to inverse problems. In quantum transport, this can be exploited to engineer an internal barrier to satisfy particular current-voltages characteristics as it will be discussed in this work.

II. MODEL

We utilize the quantum transmitting boundary model [4], [5]. Charge is injected into a 1D quantum wire from the left.

For the the physics-informed neural network the model is represented as two coupled ODEs corresponding to the real and imaginary components of the quantum wavefunction. The continuity equation is included as well; PINNs benefit from conservation law regularizations [6]. In the inverse problem, the internal potential is also a neural network. The target is encoded as a boundary condition along the domain edge.

For the differentiable simulation the wavefunction is computed on a fixed grid and transmission and current is computed with a fixed discretization. The barrier is modeled by two box functions parametrized by their position, width and height. The current-voltage characteristics are optimized with respect to the barrier parameters and the Fermi level.

A. Physics-Informed

The wavefunction is separated into its real and imaginary parts as follows:

$$\Psi = \Psi_R + i\Psi_I. \quad (1)$$

The wavenumbers corresponding to the source k_1 and drain k_2 of the device are given by:

$$k_1 = \sqrt{\frac{2m}{\hbar^2}(E - V(x = 0))}, \quad (2)$$

$$k_2 = \sqrt{\frac{2m}{\hbar^2} (E - V(x=L))}. \quad (3)$$

The following are the boundary conditions in the quasi-static approximation with current being injected from the left:

$$\left. \frac{d\Psi_R(x; E)}{dx} \right|_{x=0} = k_1 \Psi_I(0; E), \quad (4)$$

$$\left. \frac{d\Psi_R(x; E)}{dx} \right|_{x=L} = -k_2 \Psi_I(L; E), \quad (5)$$

$$\left. \frac{d\Psi_I(x; E)}{dx} \right|_{x=0} = 2k_1 - k_1 \Psi_R(0; E), \quad (6)$$

$$\left. \frac{d\Psi_I(x; E)}{dx} \right|_{x=L} = k_1 \Psi_R(L; E). \quad (7)$$

The governing equation in quantum transport is the Time-Independent Schrödinger Equation:

$$\left[-\frac{\hbar^2}{2m} \frac{d^2}{dx^2} + V(x) \right] \Psi_R(x; E) = E \Psi_R(x; E), \quad (8)$$

$$\left[-\frac{\hbar^2}{2m} \frac{d^2}{dx^2} + V(x) \right] \Psi_I(x; E) = E \Psi_I(x; E). \quad (9)$$

Where $V(0 \leq x \leq L)$ is an arbitrary total internal potential including the barrier potential (in quantum transport, $V(x \leq 0) = 0$ and $V(x \geq L) = V_0$).

The following constraint enforces the conservation of probability:

$$\frac{d}{dx} \left(\Psi_R \frac{d\Psi_I}{dx} - \Psi_I \frac{d\Psi_R}{dx} \right) = 0. \quad (10)$$

Lastly, for the inverse problem, the additional constraint enforces the transmission properties are a desired target relation, $T(E)$:

$$\frac{k_2}{k_1} |\Psi(x=L; E)|^2 = T(E). \quad (11)$$

B. Differentiable

Parametrized by height, center and width; $\vec{\theta} = (H, C, W)$, we define the barrier function, $B(x; \vec{\theta})$, with convenience functions $\text{LHS}(x; \vec{\theta})$ and $\text{RHS}(x; \vec{\theta})$ to model internal barriers as follows:

$$\text{LHS}(x; \vec{\theta} = (H, C, W)) = H \tanh \left(x - \frac{L(2C - W)}{2} \right), \quad (12)$$

$$\text{RHS}(x; \vec{\theta} = (H, C, W)) = H \tanh \left(x - \frac{L(2C + W)}{2} \right), \quad (13)$$

$$B(x; \vec{\theta}) = \frac{\text{LHS}(x; \vec{\theta}) - \text{RHS}(x; \vec{\theta})}{2}. \quad (14)$$

The total internal parametrized potential, $U(x; \vec{\phi}, E, V_0)$, is given by:

$$U(x; \vec{\phi}, E, V_0) = B_{DBL}(x; \vec{\theta}_1, \vec{\theta}_2) - V_{BIAS}(x; V_0) - E, \quad (15)$$

where $B_{DBL}(x; \vec{\phi})$ and $V_{BIAS}(x; V_0)$ are the internal barrier and bias across the device, respectively:

$$B_{DBL}(x; \vec{\phi} = (\vec{\theta}_1, \vec{\theta}_2)) = B(x; \vec{\theta}_1) + B(x; \vec{\theta}_2), \quad (16)$$

$$V_{BIAS}(x; V_0) = V_0 \frac{x}{L}. \quad (17)$$

After discretization, the Schrödinger equation for quantum transport is modelled by the following linear system:

$$(\mathcal{H} + \mathcal{U} + \mathcal{B}) \tilde{\Psi} = \tilde{\mathbf{S}}. \quad (18)$$

Using a 1D finite different method (FDM), \mathcal{H} becomes the following Hamiltonian matrix:

$$\begin{bmatrix} \alpha & -\alpha & & & \\ -\alpha & 2\alpha & -\alpha & & \\ & -\alpha & 2\alpha & -\alpha & \\ & & \ddots & \ddots & \ddots \\ & & & -\alpha & \alpha \end{bmatrix}$$

with $\alpha = \hbar^2 / (2m_e * a_n^2)$, $a_n = L / (n - 1)$ (m_e is the electron mass, \hbar is the Planck constant, L is the length of the 1D device and n is the number of FDM discretization points).

In (18), \mathcal{U} is the total internal potential (diagonal matrix after discretization):

$$\begin{bmatrix} U(x_1; \vec{\phi}, E, V_0) & & & & \\ & U(x_2; \vec{\phi}, E, V_0) & & & \\ & & \ddots & & \\ & & & \ddots & \\ & & & & U(x_n; \vec{\phi}, E, V_0) \end{bmatrix}$$

and \mathcal{B} represents the quantum transmitting boundary conditions:

$$\begin{bmatrix} -\text{BND}_1(E, V_0) & & & & \\ & 0 & & & \\ & & \ddots & & \\ & & & 0 & \\ & & & & -\text{BND}_2(E, V_0) \end{bmatrix}$$

where $\text{BND}_j(E, V_0)$ corresponds to the boundary conditions at the j th terminal of the 1D device:

$$\text{BND}_j(E, V_0) = ik_j(E, V_0) \alpha a_n. \quad (19)$$

Finally, $\tilde{\mathbf{S}}$ is the source term corresponding to the charge injected at $x = 0$:

$$\begin{bmatrix} 2\text{BND}_1(E, V_0) \\ 0 \\ 0 \\ \vdots \\ 0 \end{bmatrix}$$

and $\tilde{\Psi}$ is the discretized wavefunction vector in (18).

Using $T(E; V_0, \vec{\phi})$ defined in (11), the quantum current through the device is given as follows (at 0K) :

$$I(V_0; \vec{\Phi} = (\vec{\phi}, \mu)) = \int_{\mu-V_0}^{\mu} T(E; V_0, \vec{\phi}) dE, \quad (20)$$

where μ is the Fermi level (given) and $\vec{\Phi}$ is a vector of all parameters of interest; internal barrier parameters ($\vec{\phi} \equiv (\theta_1, \theta_2)$) and the Fermi level.

Given m desired current voltage measurements (observations), \vec{O}_m , the error, $\vec{L}(\vec{\Phi}; \vec{O}_m)$, and Loss, $\vec{\mathcal{L}}(\vec{\Phi}; \vec{O}_m)$, are given by:

$$\vec{V}_T = (V_{T1}, V_{T2}, V_{T3}, \dots, V_{Tm}), \quad (21)$$

$$\vec{I}_T = (I_{T1}, I_{T2}, I_{T3}, \dots, I_{Tm}), \quad (22)$$

$$\vec{L}(\vec{\Phi}; \vec{O}_m \equiv (\vec{I}_T, \vec{V}_T)) = I(\vec{V}_T; \vec{\Phi}) - \vec{I}_T, \quad (23)$$

$$\vec{\mathcal{L}}(\vec{\Phi}; \vec{O}_m) \equiv \frac{\vec{L}(\vec{\Phi}; \vec{O}_m) \cdot \vec{L}(\vec{\Phi}; \vec{O}_m)}{m}. \quad (24)$$

The Inverse Problem is formulated as the following optimization problem:

$$\underset{\vec{\Phi}}{\text{minimize}} \quad \mathcal{J}(\vec{\mathcal{L}}(\vec{\Phi}; \vec{O}_m)), \quad (25)$$

where $\mathcal{J}(\vec{\mathcal{L}}(\vec{\Phi}; \vec{O}_m))$ is the Jacobian of the Loss.

III. RESULTS

A. Physics-Informed

In the physics-informed case, both the wavefunction, $\Psi(x; E)$, and total internal potential, $V(x)$, are neural networks that co-optimized in the training process to reproduce a target transmission curve. The bias V_0 is taken as -0.375eV, with the internal potential fixed at each terminal; $V(x=0) = 0$ and $V(x=L) = V_0$. The network is trained on Fourier features, that is, in the Fourier domain, to suppress the effect of spectral bias. The API, SciANN [7], is used for all neural network training.

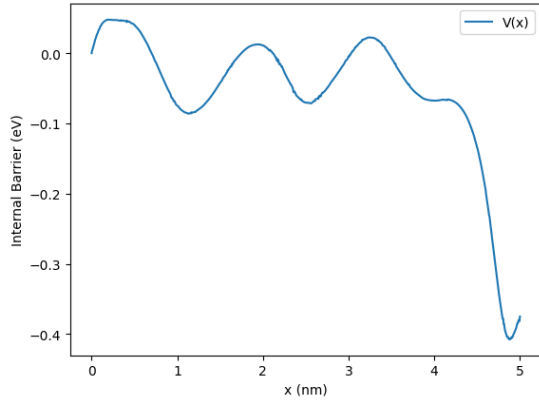


Fig. 1. Engineered internal potential.

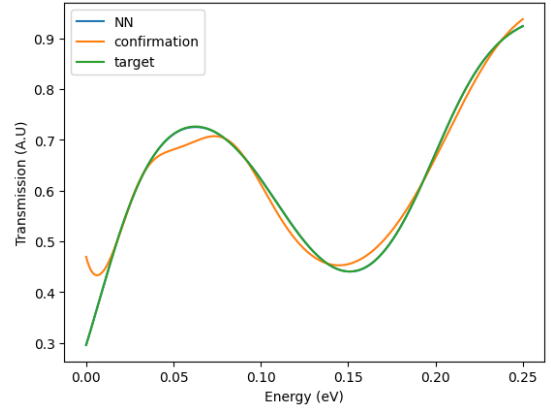


Fig. 2. Target transmission properties (green) vs. the neural network prediction (blue) and the 'confirmation' transmission properties (orange).

Fig. 1 and 2 show the optimized barrier and corresponding transmission curves, respectively. The internal potential is optimized as a neural network to satisfy the desired targeted quantum transmission curve. The history of the Loss is shown in Fig. 3. The orange curve in Fig 2 is the "confirmation" transmission curve obtained when the optimized potential in Fig 1, is passed to a finite-difference solver.

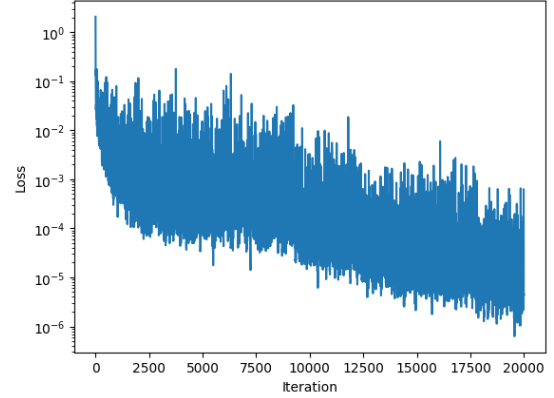


Fig. 3. History of model loss over 20,000 training iterations.

B. Differentiable

For the differentiable simulation, differentiation is implemented with JAX [8] and optimization is implemented with Optax [9]. JAX is employed due to its autovectorization functionality; `vmap()`. Computation of transmission properties and current-voltage characteristics require evaluations of continuous functions of parameters, thus it is necessary to map the linear solve over E to compute the transmission properties and to map the computation of the transmission over V to compute the current.

The Loss is computed by the functions below.

```
def TSM(E, V, theta, theta2): return k2(E, V) * \
(abs(QT(E, V, theta, theta2)) ** 2) [N-1] / \
(k1(E) + 1E-10)
```

```

def I(V,theta,theta2,uf): return np.trapz(\
np.interp(np.linspace(uf-V,uf,M2),\
np.linspace(0,uf,M),\
vmap(TSM,(0,None,None,None))\
(np.linspace(0,uf,M),V,theta,theta2)),\
np.linspace(uf-V,uf,M2))

def Loss(P): return\
((vmap(I,(0,None,None,None))\
(vT,P[0:3],P[3:6],P[6]) - iT)**2).mean()

J = jacfwd(Loss)

```

JAX employs operator overloading to differentiate through the functions $\text{Loss}(P)$, $I(V, \theta, \theta_2, u_f)$ and $\text{TSM}(E, V, \theta, \theta_2)$.

The internal potential is optimized via the training loop below where the Adabelief optimizer is utilized for its combination of adaptive learning and performance [10]:

```

optimizer = \
optax.adabelief(learning_rate=0.001)

state = optimizer.init(initial_params)
for i in range(num_iterations):
    gradient = vmap(J)(initial_params)
    updates, state = optimizer.\
    update(gradient, state, initial_params)
    updated_params = optax.\
    apply_updates(initial_params, updates)
    initial_params = updated_params

```

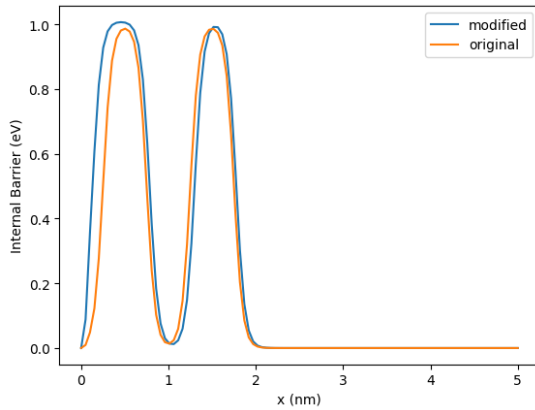


Fig. 4. Original potential (orange) vs. modified potential (blue).

Fig. 4 and 5, show the internal double barrier and current-voltage characteristics of two resonant-tunneling type devices. The 'modified' device is specified to dissipate less power and have a greater negative differential resistance than the 'original', demonstrating a plausible application in the design of low-power amplifiers [11]. The double barrier is contained within a window function to penalize barrier configurations inside the terminals; $U(x = 0) - U(x = L) \neq V_0$ is unphysical.

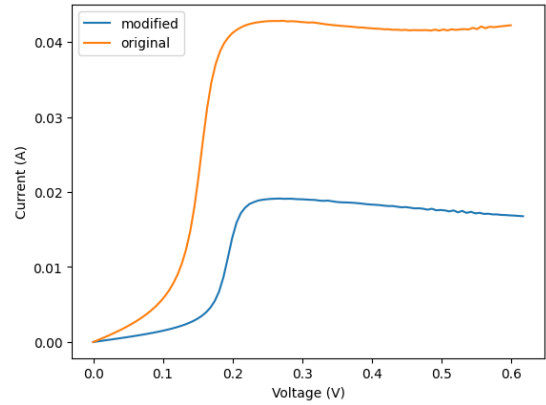


Fig. 5. Original current-voltage (orange) vs. target current-voltage (blue).

IV. CONCLUSION

A neural solver and differentiable simulation are demonstrated for inverse quantum transport. The neural solver can engineer continuous electron-wave transmission properties and the differentiable simulation can engineer current voltage relations.

Future work will focus on the inverse problem in the context of differentiable simulation due to flexibility of AD tools compatible with existing numerical algorithm paradigms. Extension to finite-element and generalizing the internal potential to a neural network is a natural next step. Incorporation of self-consistent methods are necessary to model devices in the many-body regime. Other possible applications may include multi-dimensional electron-wave devices [12].

REFERENCES

- [1] M. Raissi, P. Perdikaris, and G. E. Karniadakis, "Physics informed deep learning (part i): Data-driven solutions of nonlinear partial differential equations," 2017.
- [2] P.-Y. Chuang and L. A. Barba, "Predictive limitations of physics-informed neural networks in vortex shedding," 2023.
- [3] C. Rackauckas, Y. Ma, J. Martensen, C. Warner, K. Zubov, R. Supekar, D. Skinner, A. Ramadhan, and A. Edelman, "Universal differential equations for scientific machine learning," 2021.
- [4] C. S. Lent and D. J. Kirkner, "The quantum transmitting boundary method," *Journal of Applied Physics*, vol. 67, pp. 6353–6359, 1990.
- [5] E. Polizzi, N. B. Abdallah, O. Vanbésien, and D. Lippens, "Space lateral transfer and negative differential conductance regimes in quantum waveguide junctions," *Journal of Applied Physics*, vol. 87, pp. 8700–8706, 06 2000.
- [6] H. Wang, X. Qian, Y. Sun, and S. Song, "A modified physics informed neural networks for solving the partial differential equation with conservation laws," *Available at SSRN 4274376*, 2022.
- [7] E. Haghghat and R. Juanes, "SciANN: A keras/TensorFlow wrapper for scientific computations and physics-informed deep learning using artificial neural networks," *Computer Methods in Applied Mechanics and Engineering*, vol. 373, p. 113552, jan 2021.
- [8] J. Bradbury, R. Frostig, P. Hawkins, M. J. Johnson, C. Leary, D. Maclaurin, G. Necula, A. Paszke, J. VanderPlas, S. Wanderman-Milne, and Q. Zhang, "JAX: composable transformations of Python+NumPy programs," 2018. url: <http://github.com/google/jax>.
- [9] I. Babuschkin and K. e. a. Baumli, "The DeepMind JAX Ecosystem," 2020. url: <http://github.com/deepmind>.
- [10] J. Zhuang, T. Tang, Y. Ding, S. Tatikonda, N. Dvornek, X. Papademetris, and J. S. Duncan, "Adabelief optimizer: Adapting stepsizes by the belief in observed gradients," 2020.

- [11] J. Lee, J. Lee, and K. Yang, "Reflection-type rtd low-power amplifier with deep sub-mw dc power consumption," *IEEE microwave and wireless components letters*, vol. 24, no. 8, pp. 551–553, 2014.
- [12] E. Polizzi and N. Ben Abdallah, "Self-consistent three-dimensional models for quantum ballistic transport in open systems," *Phys. Rev. B*, vol. 66, p. 245301, Dec 2002.

APPENDIX A

TABLE OF HYPERPARAMETERS

PINNs	parameters
NN size (all)	[8X20]
n	1000
FF samples	20
FF std.dev.	1
FF mean	0
Training step	0.001
Training iterations	20000
Training samples	20000

DS	parameters
FD discretization	100
Energy Points	100
Interpolation Points	100
m	2
Search Space	5
optimizer iterations	100